PRAMANA
— journal of
physics

Vol. 71, No. 4
October 2008
pp. 819–828

Inelastic neutron scattering and lattice dynamics of minerals

NARAYANI CHOUDHURY* and S L CHAPLOT
Solid State Physics Division, Bhabha Atomic Research Centre, Mumbai 400 085, India
*Corresponding author. E-mail: dynamics@barc.gov.in

Abstract. We review current research on minerals using inelastic neutron scattering and lattice dynamics calculations. Inelastic neutron scattering studies in combination with first principles and atomistic calculations provide a detailed understanding of the phonon dispersion relations, density of states and their manifestations in various thermodynamic properties. The role of theoretical lattice dynamics calculations in the planning, interpretation and analysis of neutron experiments are discussed. These studies provide important insights in understanding various anomalous behaviour including pressure-induced amorphization, phonon and elastic instabilities, prediction of novel high pressure phase transitions, high pressure–temperature melting, etc.

Keywords. Inelastic neutron scattering; lattice dynamics; thermodynamic properties; *ab initio* calculations.

PACS Nos 25.40.Fq; 29.30.Hs; 63.20.D; 71.15.Mb

1. Introduction

An understanding of the fundamental physics of the Earth's interior requires information about the phase transitions and thermodynamic properties of key constituent mineral phases [1–10]. Information about the Earth's interior is only indirectly inferred from seismic observations. Compositional modelling based on accurate data about the structure and thermodynamic properties of minerals is essential to interpret the complex seismic data. Of particular interest is an understanding of mineral behaviour in terms of its microscopic structure and dynamics [1–15]. These characteristic properties are conveniently studied using neutron scattering-based techniques. Current generation of diffractometers and spectrometers at modern neutron sources, permit accurate determination of the structural and dynamical behaviour of minerals and have helped one to understand the high pressure–temperature crystal structures, lattice vibrations, anomalous thermodynamic behaviour, structural phase transitions, etc.

Here, we review the current status of inelastic neutron scattering and lattice dynamics of minerals. Inelastic neutron scattering measurements have been used to study key lattice dynamical properties like the phonon dispersion relations and density of states, which govern a wide range of material behaviour, including

structural phase transitions, thermodynamic properties, elasticity and melting. These, in combination with theoretical first principles calculations and atomistic simulations, have helped one to study the phonon spectra and associated physical properties of a wide variety of minerals. The neutron data have played a key role in validating theoretical models. The calculations have been fruitfully used to plan, interpret and analyse inelastic neutron scattering experiments and for the prediction of various macroscopic properties.

2. Results

The experimental INS technique has been discussed in several detailed review papers [1–3,6,7]. In table 1, we summarize selected research efforts involving inelastic neutron experiments and theoretical calculations in understanding the phonon spectra and associated thermodynamic properties of key minerals of geophysical interest. Using typical examples we review and illustrate some results of current interest [1–28]. Most of the reported theoretical studies employ the codes DISPR [29] and MOLDY [29] developed at Trombay. The first principles lattice dynamics calculations have been carried out using the code ABINIT [30].

2.1 *Zircon* ($ZrSiO_4$)

Zircon is an important mineral found in igneous rocks and sediments. Since it is a natural host for the radioactive elements uranium and thorium in the crust, it is a potential candidate for nuclear waste storage. High pressure–high temperature stability of zircon is therefore of considerable interest. A phase transition from the zircon to scheelite structure has been observed in static high pressure and shock experiments.

INS measurements of the phonon dispersion relation (PDR) of zircon [5,6] were carried out at various reactors (Dhruva [6], LLB [5]) and at the ISIS pulsed neutron source [6]. The observed INS data from reactors and spallation sources (figure 1) are in good agreement. The high symmetry of this mineral (bct, space group $I4_1/amd$, 12 atoms in the primitive cell), relative to other minerals, was well exploited for selectively measuring phonons of specific group theoretical representations. The PDR data on zircon [5] may be seen as a rare example of extensive measurements of the PDR up to 85 meV. First principles density functional perturbation theory calculations of the phonon dispersion relations were completed and found to be in agreement with the measurements [5]. The experimental data of the phonon frequencies and the crystal structure have been used to refine an interatomic potential with a lattice dynamical shell model [5]. The shell model calculations produce a very good description of the available data on the phonon density of states measured on a polycrystalline sample. The model is used further to calculate the structure, dynamics, equation of state, specific heat, thermal expansion and the Gibb's free energy as a function of pressure, in the zircon and scheelite phases. The free energy calculation reproduces the stability of the scheelite phases above 10 GPa [5]

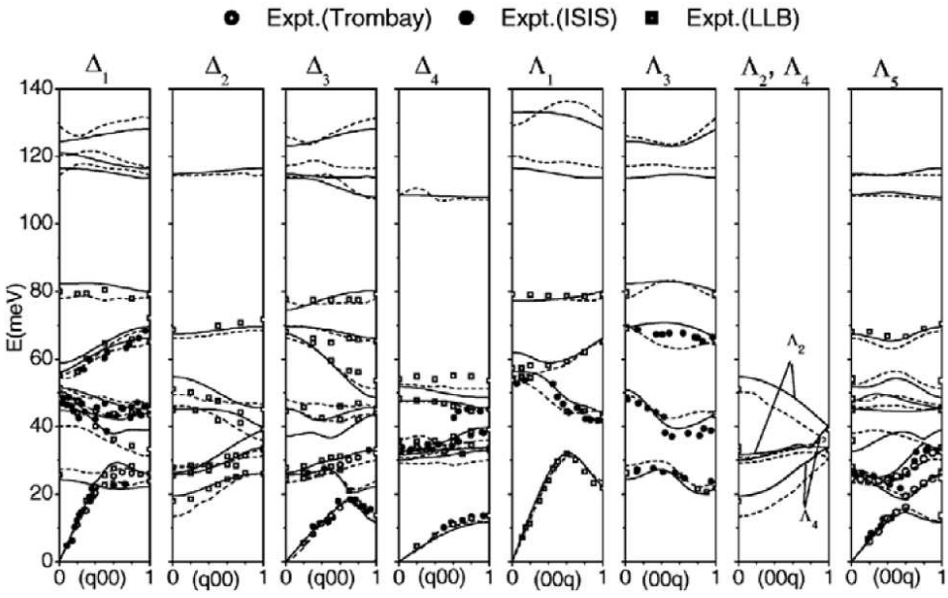

Figure 1. The experimental phonon dispersion curves in zircon [5] compared with the lattice dynamical calculations (solid lines for shell model, dashed lines for *ab initio* calculations for zircon). The open rectangles, solid circles and open circles give the phonon peaks identified in the experiments at LLB (France), ISIS ([6], UK), and Dhruva ([6], India), respectively.

as compared to the zircon phase that is in qualitative agreement with experimental observations.

2.2 *High pressure phonon softening and phase transition of α-quartz*

Silica is an important mineral occurring in the Earth's crust. Silica in its various crystalline and amorphous forms finds several industrial applications as a raw material for glasses, ceramics, production of silicon, etc. The silica polymorph α-quartz exhibits several interesting properties [4] including pressure-induced amorphization, high pressure and temperature phase transitions, anomalous elastic properties, negative Poisson ratios, soft mode behaviour, etc.

Inelastic neutron scattering measurements of the complete phonon dispersion relations of α-quartz along various high symmetry directions have been reported [16,17] and are found to be in very good agreement with DFPT first principles calculations [26] of α-quartz (figure 2). DFPT calculations [27] indicate that the phonon density of states of α-quartz with tetrahedrally coordinated silicate is significantly different from that of stishovite involving octahedrally coordinated silicon. These differences in the density of states give rise to important differences in their calculated and observed heat capacities [27].

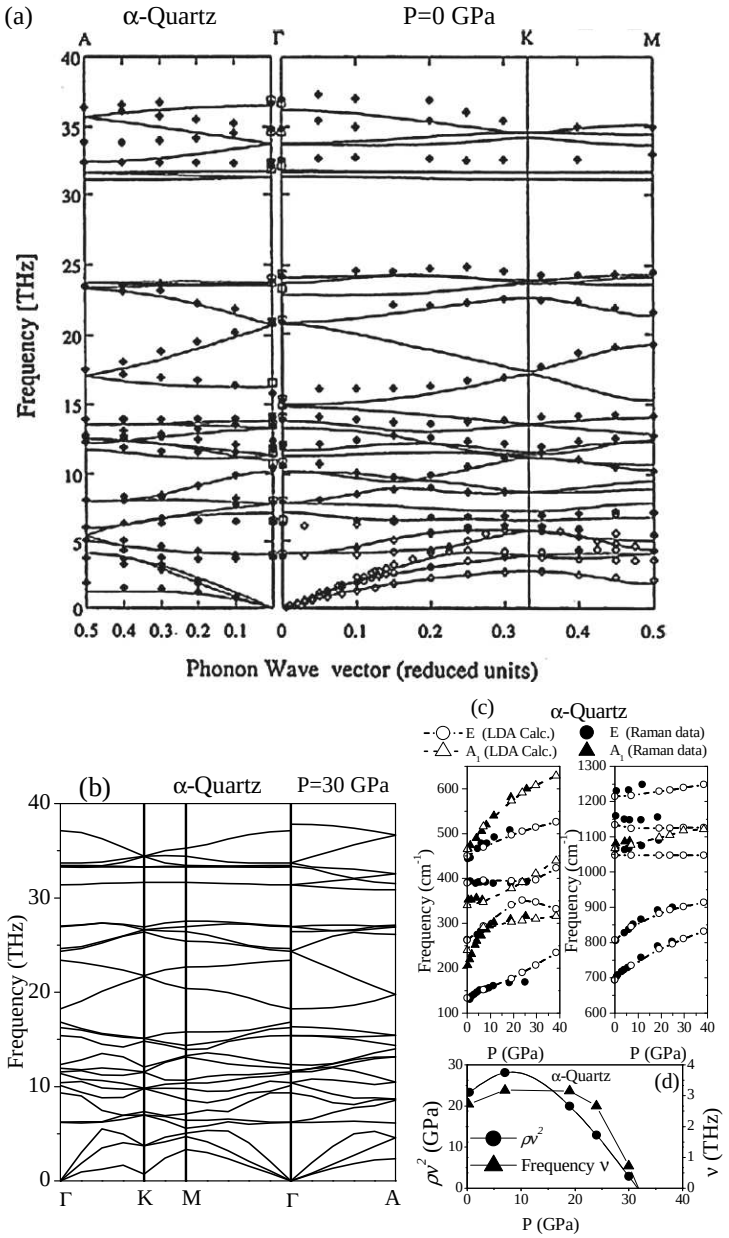

Figure 2. (**a**) The $P = 0$ phonon dispersion relations $\omega_j(\mathbf{q})$ of α-quartz (symbols give measured INS data [16,17] compared with the first principles calculations [26]). (**b**) High pressure $\omega_j(\mathbf{q})$ of α-quartz obtained via *ab initio* calculations [4] carried out using the code ABINIT [30]. (**c**) The calculated [4] long wavelength phonon frequencies compared with Raman data [31]. (**d**) The phonon and elastic instabilities of α-quartz at high pressure [4].

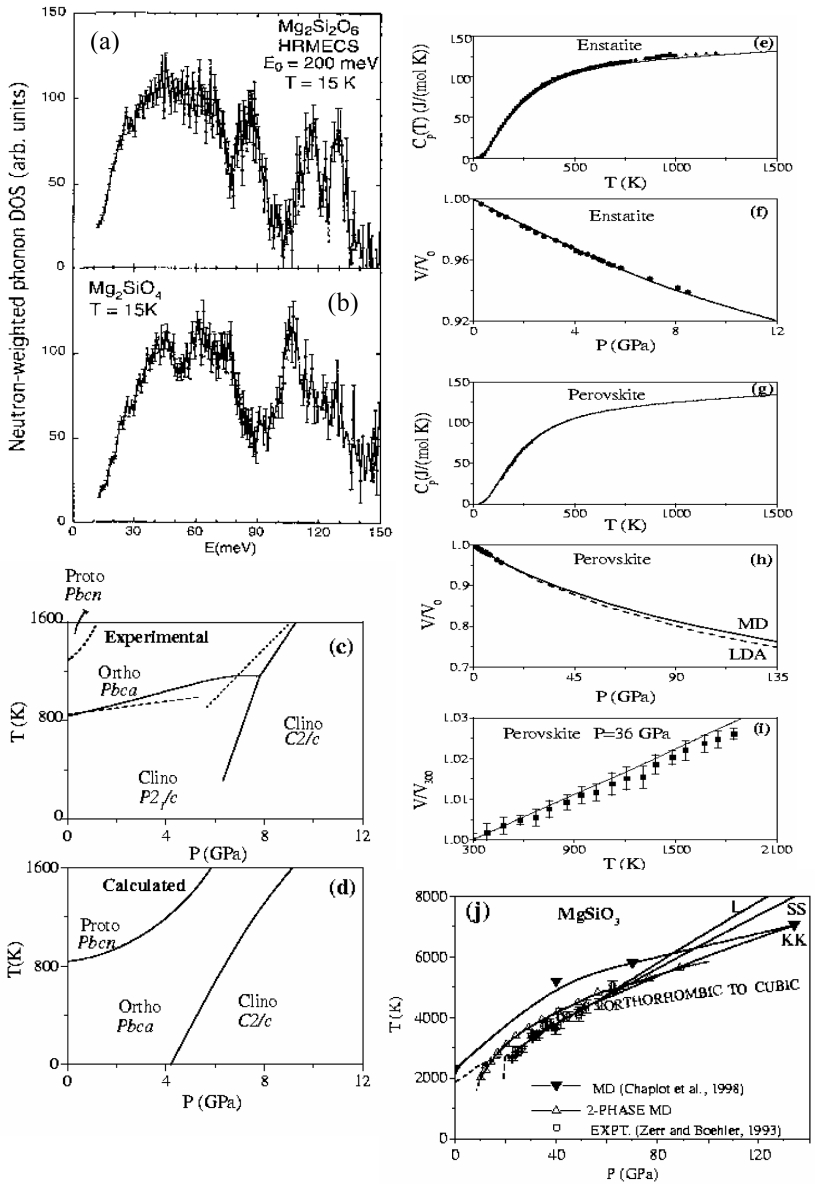

Figure 3. (**a**–**b**) The measured phonon density of states of enstatite and forsterite [14]. The INS data were used to validate interatomic potentials. The models in turn were used for calculations [10–14] of the phase diagram (**c**–**d**), high pressure and temperature thermodynamic properties (**e**–**i**) and melting (**j**) which are in good agreement with experimental data [32–43] and *ab initio* studies [42]. The two-phase MD studies of melting in (j) are from ref. [43].

Quartz amorphizes at pressures of around 18–35 GPa [4]. Although pressure-induced amorphization occurs in a variety of solids like α-quartz, coesite, ice, etc. its origins are not clearly understood. Molecular dynamics (MD) simulations using interatomic potentials fitted to first principles total energy surfaces [28] reveal pressure-induced amorphization at $P \sim 22$ GPa, in agreement with experiments. Around the amorphization pressure, α-quartz displays soft phonon modes [4] with a K-point phonon mode becoming unstable above $P = 21$ GPa. First principles DFPT calculations [4] of the phonon dispersion relations and elastic properties of α-quartz at high pressures (figure 2) confirm the K-point phonon instability at high pressure. The calculated crystal structure, equation of state and long wavelength phonon frequencies (figure 2) are found to be in good agreement with the reported high-pressure experimental data and the available first principles LDA calculations. The calculations reveal that the zone boundary (1/3, 1/3, 0) K-point phonon mode becomes unstable for pressures above $P = 32$ GPa. Around the same pressure, studies of the Born stability criteria reveal that the structure is mechanically unstable. The phonon and elastic softening (figure 2) are related to the high pressure phase transitions and amorphization of quartz and these studies suggest that the mean transition pressure is lowered under non-hydrostatic conditions. Application of uniaxial pressure results in a post-quartz crystalline monoclinic C2 structural transition [4]. This structure, intermediate between quartz and stishovite has two-thirds of the silicon atoms in octahedral coordination while the remaining silicon atoms remain tetrahedrally coordinated. This monoclinic C2 polymorph of silica, which is found to be metastable under ambient conditions, is possibly one of the several competing dense forms of silica containing octahedrally coordinated silicon. The calculated X-ray intensities of this phase compare satisfactorily with an hitherto unidentified high pressure phase of silica [4].

2.3 *The $MgSiO_3$ polymorphs enstatite and perovskite*

Enstatite is the magnesium end-member of pyroxene $(Mg_{1-x}Fe_x)SiO_3$ which is an important rock-forming silicate [10–14] and a constituent abundant in the upper mantle besides olivine $(Mg,Fe)_2SiO_4$. Enstatite has several polymorphs: orthoenstatite, protoenstatite and the low and high clinoenstatites whose structures are closely related. The basic building blocks of the enstatite polymorphs comprise of single SiO_4 chains and double MgO_6 octahedral bands. Structurally, the polymorphs are distinguished by different stacking sequences of the orientations of the MgO_6 octahedra with respect to the silicate chains. Inelastic neutron scattering measurements of the phonon density of states in polycrystalline orthoenstatite have been carried out [14]. Important structural differences involving isolated silicate tetrahedra in forsterite (Mg_2SiO_4) and silicate tetrahedral chains in enstatite give rise to distinct signatures in the phonon spectra (figure 3). The band gaps in forsterite in 90–110 meV range are bridged by the vibrations of the bridging oxygens in enstatite.

The INS data are interpreted based on lattice dynamical models employing interatomic potentials validated by X-ray diffraction, Raman, infra-red and inelastic neutron data [14]. It is worth noting that the model of interatomic potential, once

tested satisfactorily, can be used to provide microscopic insights on a wide variety of complex phenomena. The computed thermodynamic properties of the $MgSiO_3$ polymorphs enstatite and perovskite (figure 3), namely, the specific heat, equation of state and thermal expansion at high pressure and temperature are in excellent agreement with the reported experimental data [11].

The computed phase diagram of enstatite obtained by comparing the Gibbs free energies of various phases [10] is found to be in qualitative agreement with experiments (figure 3). While there is some ambiguity from experiments about whether the orthoenstatite or the $P2_1/c$-clinoenstatite is the stable ambient phase, lattice dynamical calculations predict essentially similar ambient state free energies for the two phases [10]. Detailed lattice dynamics calculations indicate that the phonon density of states as a function of pressure of the various enstatite polymorphs ortho-, proto-, $P2_1/c$ (low) clinoenstatite and $C2/c$ (high) have gross similarities [10] and are in overall agreement with the measured phonon density of states of orthoenstatite. In the low frequency region, the phonon density of states of the proto-phase is shifted to lower frequencies, resulting in a higher vibrational entropy of the proto-phase as compared to the ortho-phase. The lowering of the low frequency density of states in the proto-phase is consistent with the observed softening of the elastic constant C_{55} in the proto-phase as compared to orthoenstatite.

Molecular dynamics studies using these potentials have been very useful in understanding the high pressure–temperature phase transitions of enstatite [11]. With increasing pressure, enstatite (with silicon in tetrahedral coordination) [11] first transforms to a new novel five-coordinated silicon phase and then to the lower-mantle perovskite phase involving six-coordinated silicon atoms. Although the occurrence of crystalline five-coordinated silicate phases is somewhat rare, the new intermediate phase obtained through the simulations is found to be crystalline. The calculated seismic velocities and densities [11] across the phase transitions for a pure $MgSiO_3$ mantle were overall in good agreement with preliminary reference earth model estimates based on seismic and other data. These MD studies [11] suggest that the major discontinuities between the upper mantle, transition zone, and the lower mantle could arise partially due to the changes in the silicon coordination. The simulations have enabled a microscopic visualization of the key mechanisms of these transitions and provide useful insights about the variations in the vibrational properties due to these changes in silicate coordination.

Another important application of these potentials was to understand the high pressure melting [12] in $MgSiO_3$ perovskite (figure 3). The MD simulations of $MgSiO_3$ perovskite revealed an orthorhombic to cubic transition accompanied by a sharp increase in diffusion of the O atoms. The phase transition and melting temperature was found to depend sensitively on the level of defects in the solid [12]. At pressures of the Earth's lower mantle, the transition is found to occur at temperatures substantially higher than the mantle temperatures.

3. Conclusions

A combination of inelastic neutron scattering experiments and lattice dynamics first principles and atomistic calculations has been very useful in providing microscopic

Table 1. Selected list of minerals for which inelastic neutron scattering measurements of phonon dispersion relations $\omega_j(\mathbf{q})$ and/or density of states $g(\omega)$ have been measured [1–25]. In most of these studies, lattice dynamics calculations have been used for the planning, analysis and interpretation of experimental neutron data and for prediction of various microscopic and macroscopic thermodynamic properties.

Material names	INS expt. $\omega_j(\mathbf{q})$	INS expt. $g(\omega)$
Olivine [1–3,8]		
Forsterite (Mg_2SiO_4) [8]	BNL	ANL
Fayalite (Fe_2SiO_4)	BNL	ANL
Pyroxene/enstatite/perovskite ($MgSiO_3$) [1–3,10–14]		
Orthoenstatite* [14]		ANL
Protoenstatite* [13]		
Low-clinoenstatite		
High-clinoenstatite		
$MgSiO_3$ perovskite		
Aluminium silicate (Al_2SiO_5) [1–3,7]		
Sillimanite [7]	ORNL	RAL
Andalusite [7,18]	Dhruva, PSI	
Kyanite		RAL
Garnets [6,19–21]		
Almandine [6]		ANL
Pyrope [6,19,20]	RAL	RAL
Grossular [21]		RAL
Spessartine		
Zircon structured compounds		
Zircon ($ZrSiO_4$) [5,6]	Dhruva, RAL, LLB	ANL
$LuPO_4$, $YbPO_4$, etc. [15]	LLB	ANL
Oxides/carbonates		
α-Quartz (SiO_2) [4,16,17]	ILL	
Quartz structured $FePO_4$, $GaPO_4$, $AlPO_4$ [6]		ANL
Sapphire (α-Al_2O_3) [25]	ILL	
α-Cr_2O_3 [22]	ILL	
Calcite ($CaCO_3$) [23,24]	NRU	
Rhodochrosite ($MnCO_3$) [7]	Dhruva	Dhruva
Na_2CO_3 [7]		Dhruva
Zirconia (ZrO_2) [9]		Dhruva
Yttria (Y_2O_3) [9]		Dhruva

ANL – Argonne National Laboratory, USA; RAL – Rutherford Appleton Laboratory, UK; BNL – Brookhaven National Laboratory, USA; ORNL – Oak Ridge National Laboratory, USA; LLB – Laboratoire Léon Brillouin, Saclay, France; Dhruva – Dhruva Reactor, Bhabha Atomic Research Centre, India; PSI – Paul-Scherrer-Institut, Switzerland; ILL – Institut Laue Langevin, France; NRU – NRU Reactor, Chalk River, Canada.

*Polarized single crystal Raman spectroscopic measurements [13,14] were also carried out at the University of Washington, USA.

insights into the characteristic phonon spectra of a wide variety of minerals. The INS data have been used to validate models that in turn have helped one to study their thermodynamic properties and phase transitions at extreme conditions of pressure and temperature. These studies shed light on various anomalous behaviours

of minerals including pressure-induced amorphization, phonon and elastic instabilities, novel high pressure phase transitions, high pressure–temperature melting, etc. The integration of neutron scattering experiments with theoretical simulation methods [1–14] have been extremely successful in providing microscopic insights relevant to high-pressure mineral and materials sciences, seismology, geochemistry, petrology, etc. and provides a new window to explore planetary interiors.

References

[1] N Choudhury and S L Chaplot, in: *Neutrons in earth, energy and environment* edited by L Liang, R Rinaldi and H Schober (Springer, 2009) pp. 145–188 and references therein

[2] S L Chaplot, N Choudhury, S Ghose, M N Rao, R Mittal and P Goel, *Euro. J. Mineral.* **14**, 291 (2002) and references therein

[3] N Choudhury, S L Chaplot, S Ghose, M N Rao and R Mittal, in: *Energy modelling in minerals*, *European Mineralogical Union Notes (EMU Notes)* edited by C M Gramaccioli (Eötvös Publishers, Budapest, Hungary, 2002) Vol. 4, pp. 211–243 and references therein

[4] N Choudhury and S L Chaplot, *Phys. Rev.* **B73**, 094304-1-11 (2006)

[5] S L Chaplot, L Pintschovius, N Choudhury and R Mittal, *Phys. Rev.* **B73**, 094308-1-8 (2006)

[6] R Mittal, S L Chaplot and N Choudhury, *Prog. Mater. Sci.* **51**, 211 (2006) and references therein

[7] Mala N Rao, R Mittal, Narayani Choudhury and S L Chaplot, *Pramana – J. Phys.* **63**, 73 (2004) and references therein

[8] K R Rao, S L Chaplot, N Choudhury, S Ghose, J M Hastings, L M Corliss and D L Price, *Phys. Chem. Mineral.* **16**, 83 (1988)

[9] P Bose, R Mittal, S L Chaplot and N Choudhury, this volume

[10] N Choudhury and S L Chaplot, *Solid State Commun.* **114**, 127 (2000)

[11] S L Chaplot and N Choudhury, *Am. Mineral.* **86**, 752 (2001)

[12] S L Chaplot and N Choudhury, *Am. Mineral.* **86**, 195 (2001)

[13] S Ghose, N Choudhury, S L Chaplot, C P Chowdhury and S K Sharma, *Phys. Chem. Minerals* **20**, 469 (1994)

[14] N Choudhury, S Ghose, C P Chowdhury, C K Loong and S L Chaplot, *Phys. Rev.* **B58**, 756 (1998)

[15] R Mittal, S L Chaplot, N Choudhury and C K Loong, *J. Phys. Condens. Matter* **19**, 446202 (2007)

[16] D Strauch and B Dorner, *J. Phys. Condens. Matter* **5**, 6149 (1993)

[17] H Schober *et al*, *J. Phys. Condens. Matter* **5**, 6155 (1993)

[18] B Winkler and W Buehrer, *Phys. Chem. Minerals* **17**, 453 (1990)

[19] G Artioli, A Pavese and O Moze, *Am. Mineral.* **81**, 19 (1996)

[20] A Pavese, G Artioli and O Moze, *Euro. J. Mineral.* **10**, 59 (1998)

[21] J Zhao, P H Gaskell, L Cormier and S M Bennington, *Physica* **B241**, 906 (1998)

[22] T May, D Strauch, H Schober and B Dorner, *Physica* **B234–236**, 133 (1997)

[23] E R Cowley and A K Pant, *Phys. Rev.* **B8**, 4795 (1973)

[24] M T Dove, M E Hagen, M J Harris, B M Powell, U Steigenberger and B Winkler, *J. Phys. Condens. Matter* **4**, 2761 (1992)

[25] H Schober, D Strauch and B Dorner, *Z. Phys.* **B92**, 273 (1993)

[26] X Gonze, J C Charlier, D C Allan and M P Teter, *Phys. Rev.* **B50**, 13035 (1994)

[27] C Lee and X Gonze, *Phys. Rev.* **B51**, 8610 (1995)
[28] S L Chaplot and S K Sikka, *Phys. Rev. Lett.* **71**, 2674 (1993)
[29] S L Chaplot, unpublished
[30] X Gonze, J-M Beuken, R Caracas, F Detraux, M Fuchs, G-M Rignanese, L Sindic, M Verstraete, G Zerah, F Jollet, M Torrent, A Roy, M Mikami, Ph Ghosez, J-Y Raty and D C Allan, *Comput. Mater. Sci.* **25**, 478 (2002)
[31] R J Hemley, in: *High pressure research in mineral physics* edited by M H Manghnani *et al* (Terra Scientific, 1997) p. 233
[32] A Zerr and R Boehler, *Science* **262**, 553 (1993)
[33] R J Angel and D A Hugh-Jones, *J. Geophys. Res.* **B99**, 19777 (1994)
[34] R E G Pacalo and T Gasparik, *J. Geophys. Res.* **B95**, 15853 (1990)
[35] M Kanazaki, *Phys. Chem. Mineral.* **17**, 726 (1991) and references therein
[36] K M Krupka, B S Hemingway, R A Robie and D M Kerrick, *Am. Mineral.* **70**, 261 (1985)
[37] R J Angel and D A Hugh Jones, *J. Geophys. Res.* **B99**, 19777 (1994)
[38] L Thieblot, C Tequi and P Richet, *Am. Mineral.* **84**, 848 (1999)
[39] M Akaogi and E Ito, *Geophys. Res. Lett.* **20**, 105 (1993)
[40] H K Mao, R J Hemley, Y Fei, J F Shu, L C Chen, A P Jephcoat and Y Wu, *J. Geophys. Res.* **B96**, 8069 (1999)
[41] N Funamori and T Yagi, *Geophys. Res. Lett.* **20**, 387 (1993)
[42] R M Wentzcovitch, J L Martins and G D Price, *Phys. Rev. Lett.* **70**, 3947 (1993)
[43] A B Belonoshko, *Am. Mineral.* **86**, 193 (2000)